Tetrahedron: *Asymmetry* 21 (2010) 2859–2867

Contents lists available at ScienceDirect

Tetrahedron: *Asymmetry*

journal homepage: www.elsevier.com/locate/tetasy

Novel tetrahydroisoquinoline based organocatalysts for asymmetric Diels–Alder reactions: insight into the catalytic mode using ROESY NMR and DFT studies

Tricia Naicker [a], Katja Petzold [b], Thishana Singh [c], Per I. Arvidsson [a,d,e], Hendrik G. Kruger [b], Glenn E. M. Maguire [b], Thavendran Govender [a,*]

[a] *School of Pharmacy and Pharmacology, University of KwaZulu-Natal, Durban Private Bag 4000, South Africa*
[b] *School of Chemistry, University of KwaZulu-Natal, Durban Private Bag 4000, South Africa*
[c] *Department of Chemistry, Durban University of Technology, Durban Private Bag 4000, South Africa*
[d] *Organic Pharmaceutical Chemistry, Department of Medicinal Chemistry, Uppsala Biomedical Centre, Uppsala University, Box 574, SE-751 23 Uppsala, Sweden*
[e] *Discovery CNS & Pain Control, AstraZeneca R&D Södertälje, S-151 85 Södertälje, Sweden*

ARTICLE INFO

Article history:
Received 28 October 2010
Accepted 5 November 2010
Available online 21 December 2010

ABSTRACT

For the first time an organocatalyst bearing a secondary nitrogen within a cyclohexane ring has been evaluated in the asymmetric Diels–Alder reaction. This organocatalyst is also the first of its kind based on a (1*R*,3*S*)-6,7-dimethoxy-1-phenyl-1,2,3,4-tetrahydroisoquinoline backbone. These catalysts were tested over a range of dienes and dienophiles and displayed promising chemical conversions of up to 100% with up to 64% ee with triflic acid as the cocatalyst. Density functional theory computational studies and 2D NMR spectroscopy were used to determine the structure of the intermediate iminium ion formed between the most efficient catalyst and cinnamaldehyde. The reaction profile for each of the four possibilities in this reaction were calculated and it was found that the iminium intermediate leading to the major product is higher in energy but kinetically preferred. The activation energies of all possible reaction paths were calculated and the results correlated with the observed products. These experiments revealed that the presence of both (*E*)- and (*Z*)-isomers of the cinnamaldehyde were contributing factors for the low enantioselectivity of the reaction products.

1. Introduction

In the last decade there has been an explosive growth in the field of organocatalysis and it has emerged as a powerful method for accelerating various asymmetric transformations.[1–3] Within this topic, the in situ generation of iminium and enamine intermediates using chiral amines (aminocatalysis) to facilitate the catalysis of carbonyl transformations has received a tremendous amount of interest from several research groups.[4–7] Significant contributions from the groups of List, MacMillan and JØrgensen have reported the use of proline (i), imidazolinone (ii) and diaryl prolinols (iii) as successful chiral organocatalysts, respectively (see Fig. 1).[8–10]

All of these organocatalysts consist of five membered heteroatom rings and were evaluated for numerous important enantioselective reactions such as Diels–Alder cycloadditions, Michael additions, Mannich and Henry reactions. The iminium activation of carbonyl compounds using secondary amines (the organocatalyst) allows for lowering of the lowest unoccupied molecular orbital (LUMO), thus emulating classical Lewis acid catalysts.[8] The principle behind iminium activation is based on the reversible condensation between a secondary amine and an unsaturated aldehyde or ketone substrate to form a positively charged iminium intermediate. This results in a redistribution of the π-electron density from the double bond of the substrate towards the iminium cation. This lowers the energy of the LUMO on the unsaturated π-system and the iminium ion intermediate facilitates nucleophilic attack on the substrate.[5]

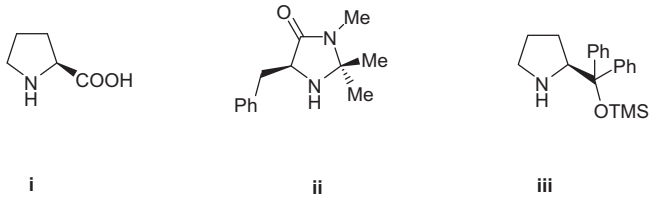

i ii iii

Figure 1. Some examples of successful secondary amine organocatalysts.

The tetrahydroisoquinoline (TIQ) molecule and its derivatives have been widely investigated due to their biological and pharmaceutical properties.[11–14] Due to our ongoing pursuit to establish

* Corresponding author.
E-mail address: govenderthav@ukzn.ac.za (T. Govender).

0957-4166/$ - see front matter © 2010 Elsevier Ltd. All rights reserved.
doi:10.1016/j.tetasy.2010.11.010

novel chiral catalysts,[15–17] and L-DOPA being commercially available, this class of compounds represented an attractive skeleton for a source of chirality. There are only a few reports that utilise the TIQ backbone as a catalyst precursor.[18–21] From these reports, only studies performed by Stingl et al.[21] and Basavaiah et al.[18] made use of a TIQ derivative as an organocatalyst in borane-mediated hydrogenation reactions. Given our recent success with TIQ based ligands for catalytic asymmetric transfer hydrogenation of prochiral ketones,[22,23] Henry reactions[24] and hydrogenation of olefins,[25] we decided to expand the potential of TIQ derivatives as organocatalysts. On route to the synthesis of a novel organocatalyst bearing the TIQ framework that would potentially behave as a bifunctional organocatalyst we discovered that one of its precursors was able to form an iminium ion. This was unexpected; secondary amines that are part of five-, rather than six-, membered ring systems are known to be more efficient catalysts for enamine catalysis,[26] and to the best of our knowledge no previous report has shown that six-membered ring amines have been successful for activating α,β-unsaturated aldehydes or ketones through iminium ion formation. This sparked our interest to further investigate this compound and its derivatives for application in reactions known to proceed via iminium activation. Herein, we report the evaluation of novel organocatalysts **1–9** in the asymmetric Diels–Alder cycloaddition between α,β-unsaturated aldehydes and cyclopentadiene. This is the first report of a chiral organocatalyst with the tetrahydroisoquinoline backbone that contains two stereogenic centres.

2. Results and discussion

2.1. Catalyst synthesis

Compounds **5**, **8** and **9** (Fig. 2) are novel, whereas the syntheses of the remaining compounds have been reported in the literature for other applications. However, this is the first report of these derivatives as organocatalysts. Based on the simplicity of the structure, TIQ catalysts **1** and **2** were the first to be synthesized according to a literature procedure from (*S*)-phenylalanine.[27] Thereafter the more complex TIQ derivatives **3**–**5** were derived from L-DOPA **10** (Scheme 1). We recently reported a modification to the literature procedure for compound **11**.[22] L-DOPA **10** was treated with benzaldehyde in the presence of K_2CO_3 and aqueous ethanol to afford the *trans*-substituted derivative **11**, and the relative configuration was confirmed by comparison to the proton NMR spectral data reported by Aubry et al. who elucidated both diastereomers of **11**.[28] This compound was N-protected with benzyl chloroformate (Cbz) and then methylated at the phenolic and carboxylic acid positions to yield **12**. This was achieved by refluxing the compound in acetone in the presence of Me_2SO_4 and $KHCO_3$.[29] Deprotection of the Cbz group furnished catalyst **4**.

Hydrolysis of the ester group in **4** afforded the acid derivative **3** and catalyst **5** was then obtained by simple esterification of **3** with thionyl chloride in isopropanol. Notably, catalysts **3**–**5** and **7**–**9** possess a second stereogenic centre and could not be synthesized from

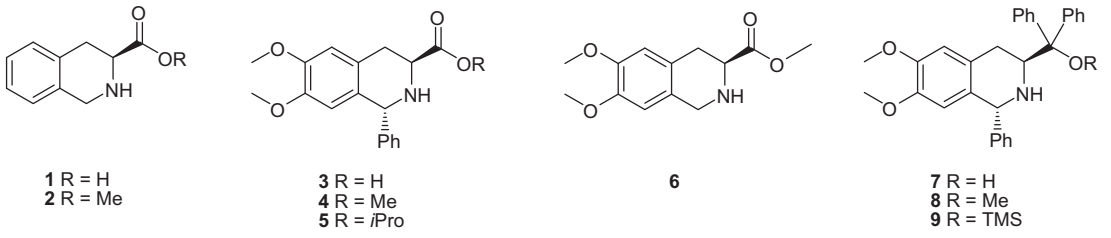

Figure 2. Catalysts evaluated for the Diels–Alder reaction.

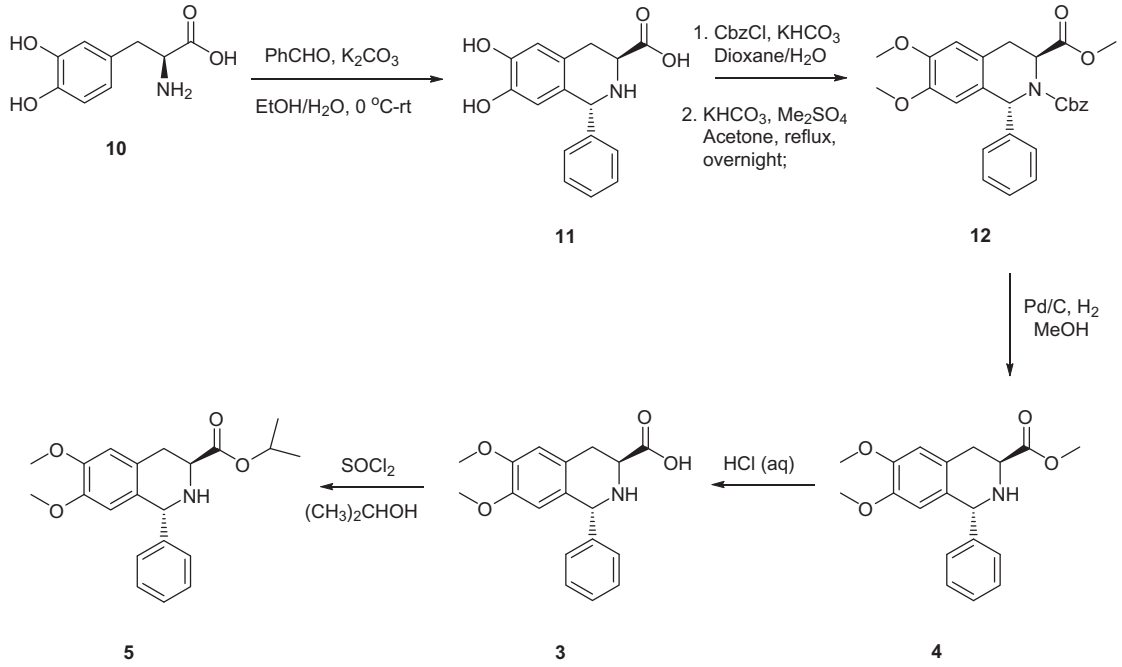

Scheme 1. Synthetic route to catalysts **3**–**5**.

phenylalanine as it was essential to employ the activated aromatic group of L-DOPA to facilitate the cyclisation. Hence, methylation of the free phenolic hydroxyl groups had to be done after cyclization in order to simplify the synthesis. In order to test the effect of these methoxy groups on the reactivity of the catalysts, derivative **6** was synthesized by a literature procedure (scheme not shown) from L-DOPA and formaldehyde followed by our modified methylation procedure for the hydroxyl and acid positions.[30] Given the success of diaryl proline derivatives as organocatalysts[31] we synthesized the six membered ring TIQ analogues **7**–**9**. In order to introduce the phenyl groups, the secondary amine **4** was first benzyl protected to give **13**, after which a Grignard reaction with phenyl magnesium bromide afforded **14**. Deprotection of **14** (Scheme 2) resulted in the formation of catalyst **7**.

Derivative **14** was then treated with NaH followed by MeI to yield the diphenyl methoxy *N*-benzyl protected compound **15,** which underwent debenzylation to give catalyst **8**. Catalyst **9** was obtained by the hydroxyl protection of **7** using trimethylsilyl trifluoromethanesulfonate.[32]

2.2. Reactions of catalysts

As a model, we investigated the reaction between cinnamaldehyde **16** and cyclopentadiene **17** in the presence of various tetrahydroisoquinoline derivatives **1**–**9** as potential catalysts (Table 1). Organocatalysts tested for this reaction have been shown to react well in either methanol or acetonitrile/water mixtures.[8,33] Performing the reaction with our catalysts in methanol did show a slightly higher conversion than acetonitrile, nevertheless, acetonitrile was chosen as the solvent since it avoids hydrolysis of the dimethyl-acetal formed when methanol is used and thus, greatly simplifies the workup.

From the TIQ catalysts **1** and **2** the ester derivative **2** showed a higher conversion than the acid derivative **1** (entries 1 and 2). Thereafter, it was decided to test the TIQ derivatives that contained a second stereogenic centre (entries 3 and 4). At that point, compound **4** emerged as the most reactive catalyst amongst **1**–**4** (entry 4). It appeared logical to substitute the methyl ester of compound **4** with a more bulky group in the hope of increasing the enantiomeric excess of the reaction products; in this case an isopropyl ester **5** was used (entry 5). However, this had an insignificant effect on the enantioselectivity. In order to evaluate if the higher conversion rate (cf. the acid derivatives **1** and **3** (53% and 67% conversion after 24 h, respectively) and the methyl esters **2** and **4** (67% and 73% conversion, respectively) was due to the introduction of the phenyl ring at the carbon adjacent to the nitrogen or the introduction of the methoxy groups, catalyst **6** was synthesized and tested (entry 6). It was clear that the methoxy groups were not responsible for the increased conversion. The activity and selectivity of catalysts **3**–**5** compared to that of catalyst **1**–**2** were then attributed to the electron withdrawing nature of the phenyl ring, which increases the acidity of the nitrogen hence favoring iminium formation. To further establish if this was the case, we attempted the reaction with pipecolic acid as the catalyst as well, but obtained

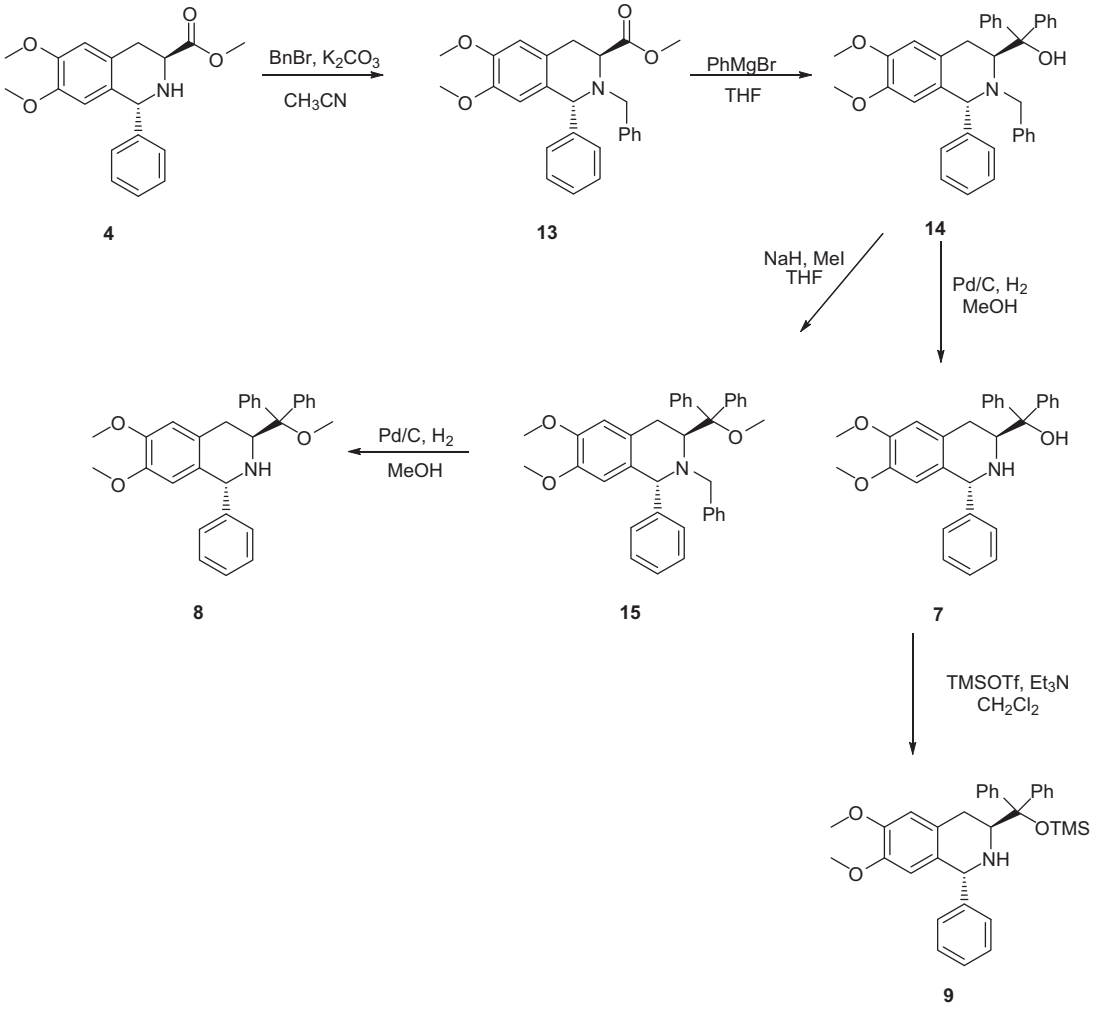

Scheme 2. Synthetic route to catalysts **7**–**9**.

Table 1
Organocatalysed [4+2] cycloaddition between *trans*-2-cinnamaldehdye **16** and cyclopentadiene **17** to give cycloaddition products *exo*- and *endo*-**18**[a]

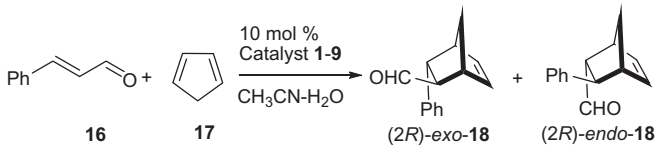

Entry	Catalyst	Conv. (%) 24 h	Conv. (%) 48 h	ee (%) *exo*-**18**[b]	ee (%) *endo*-**18**[b]	*exo*:*endo*[c]
1	**1**	53	78	47 (2*R*)	48 (2*R*)	2:1
2	**2**	67	94	43 (2*R*)	50 (2*R*)	2:1
3	**3**	67	90	44 (2*R*)	50 (2*R*)	2:1
4	**4**	73	94	45(2*R*)	51 (2*R*)	2:1
5	**5**	73	94	46 (2*R*)	57 (2*R*)	2:1
6	**6**	58	62	36 (2*R*)	36(2*R*)	2:1
7	**7**	<5	–	–	–	2:1
8	**8**	<5	–	–	–	2:1
9	**9**	<5	–	–	–	2:1

[a] Conditions: 3.0 equiv of diene, 1.0 equiv of dienophile, 0.1 equiv of catalyst and 0.1 equiv of HCl (37%) in 475 μl of CH_3CN and 25 μl of H_2O, all reactions were performed in duplicate.
[b] Determined by GC analysis using a chiral capillary column and absolute and relative configurations were determined by correlation of GC retention times. The absolute and relative configurations were initially determined by correlation to known compounds.
[c] The product ratios were determined by ^1H NMR recorded at ambient temperature.

only low (<10%) conversions, even in the presence of an acidic co-catalyst (vide supra).

Given the success of the diaryl proline analogues as organocatalysts[31] we synthesized the TIQ derivatives **7–9** to be tested on the model reaction. The molecules showed very low conversion rates (entries 7–9). Evidence for iminium formation from catalysts **7–9** with cinnamaldehyde was confirmed with proton NMR spectroscopy. The low conversion could be due to one of two reasons, first, the diene could not attack the dienophile or second the reaction product is not released from the catalyst.

As with other organocatalysts tested for this reaction, an acid co-catalyst proved to be necessary. Therefore, we investigated the effect of varying the type of acid with catalysts **2** and **4** (Table 2). The trend observed was that the conversion is proportional to the pK_a of the acids. Using a sterically large acid did not influence the enantioselectivity (entry 2). The triflic counterion gave optimal conversion and enantioselectivity (entry 5). The possibility of such a strong acid catalyzing this Diels–Alder reaction and compromising the enantioselectivity by a competing achiral process has been thoroughly investigated by Lemay et al.[34] From their study it was concluded that triflic acid was not detrimental to the selectivity of the reaction.

Having optimized the conditions for the system, the scope of these new TIQ based catalysts using various other dienophiles and dienes was investigated (Table 3).

A range of aliphatic dienophiles including electron-withdrawing and -donating group substituents on the cinnamaldehyde aryl ring were tested with cyclopentadiene (entries 1–6). All substrates gave excellent conversion with the exception of 4-methoxy cinnamaldehyde. The TIQ catalyst also proved to be efficient when varying the diene (entries 7 and 8) producing excellent conversion and facial selectivity (entry 8) but unfortunately poor enantioselectivity.

2.3. Structural elucidation of the iminium ion intermediate by NMR spectroscopy and computational chemistry

Seebach et al. have thoroughly investigated the structural characterization of reactive iminium ion intermediates derived from proline, diphenyl prolinol and imidazolidinones with cinnamaldehyde, employing X-ray diffraction, NMR spectroscopy and density functional theory (DFT) computational studies.[35–38] They have concluded that (*E*)- and (*Z*)-isomers are possible for the iminium ion intermediates as illustrated in Scheme 3.

We then decided to follow a similar methodology to elucidate the structure of the iminium ion formed between cinnamaldehyde and our catalyst **4**. We recently reported the X-ray crystal structures of precursors to catalyst **4** and **7,** which revealed that the N-containing six membered ring could exist either as a half boat or half chair form, respectively.[39,40] Based on these forms of the

Table 2
Organocatalysed [4+2] cycloaddition between *trans*-2-cinnamaldehdye **16** and cyclopentadiene **17** using catalyst **2** and **4** in CH_3CN with different acids[a]

Entry	Catalyst	Acids	Conv. (%) 24 h	Conv. (%) 48 h	ee (%) *exo*-**18**[b]	ee (%) *endo*-**18**[b]	*exo*:*endo*[c]
1	**2**	HCl	71	93	47 (2*R*)	48 (2*R*)	2:1
2	**2**	*p*-TsOH	83	98	43 (2*R*)	50 (2*R*)	2:1
3	**2**	TFA	75	92	43 (2*R*)	50 (2*R*)	2:1
4	**2**	CH_3SO_2H	77	91	46 (2*R*)	46 (2*R*)	2:1
5	**2**	TfOH	100	–	43 (2*R*)	51 (2*R*)	2:1
6	**4**	HCl	73	90	45 (2*R*)	51 (2*R*)	2:1
7	**4**	*p*-TsOH	72	90	48 (2*R*)	47 (2*R*)	2:1
8	**4**	TFA	65	90	49 (2*R*)	55 (2*R*)	2:1
9	**4**	CH_3SO_2H	70	90	47 (2*R*)	42 (2*R*)	2:1
10	**4**	TfOH	95	–	47 (2*R*)	57 (2*R*)	2:1
11	**4**	TfOH	85 (12 h)	–	47 (2*R*)	57 (2*R*)	2:1

[a] Conditions: 3.0 equiv of diene, 1.0 equiv of dienophile, 0.1 equiv of catalyst and 0.1 equiv of acid in 475 μl of CH_3CN and 25 μl of H_2O, all reactions were performed in duplicate.
[b] Determined by GC analysis using a chiral capillary column and the absolute and relative configuration were determined by correlation of GC retention times. The absolute and relative configuration were initially determined by correlation to known compounds.
[c] The product ratios were determined by ^1H NMR recorded at ambient temperature.

Table 3
Organocatalysed Diels–Alder cycloadditions between various dienophiles and dienes utilising catalyst **4** and TfOH in CH_3CN[a]

Entry	Dienophile	Diene	Conv. (%) 12 h	ee (%) *exo*[b]	ee (%) *endo*[b]	*exo*:*endo*[c]
1	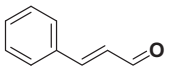		85 (55[d])	47 (64[d])	57 (59)	2:1
2	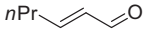		100	22	*rac*	1:1
3	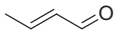		100	*rac*	4	1.2:1
4			100	5	10	3.5:1
5	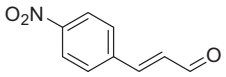		100	35	42	2:1
6	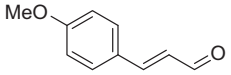		40	52	4	1.6:1
7			100	30	–	–
8			100	*rac*	38	7:1

[a] Conditions: 3.0 equiv of diene, 1.0 equiv of dienophile, 0.1 equiv of catalyst and 0.1 equiv of acid in 475 μl of CH_3CN and 25 μl of H_2O.
[b] Determined by GC analysis using a chiral capillary column.
[c] The product ratios were determined by ^1H NMR recorded at ambient temperature.
[d] Reaction carried out at 0 °C and conversion tested after 36 h.

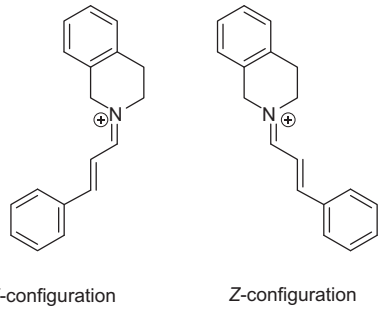

Scheme 3. Possible isomers of the iminium ion formed between *trans*-2-cinnamaldehyde and tetrahydroisoquinoline.

catalyst together with the possibility of the (*E*)- and (*Z*)-isomers of the reacting aldehyde, the structure of the iminium ion formed between cinnamaldehyde and catalyst **4** (Fig. 3) were examined. The four possibilities A–D were computationally studied utilising DFT calculations and are presented in Figure 3.

The calculations indicated that intermediate **B** had the lowest energy conformation. NMR spectra of cinnamaldehyde in the presence of catalyst **4** were obtained to determine the geometry of cinnamaldehyde in the resulting complex. Specific features from the ROESY spectrum revealed that forms **A** and **B** coexist in the solution phase which corresponds to the (*E*)- and (*Z*)-isomers around the C=N bond, respectively. Formation of imines is reversible at room temperature,[8] therefore, it is possible for **A** and **B** to exist in equilibrium. The presence of these structures was inferred from the ROESY correlations of protons H1 and H9 to the HB protons on the substrate (see Fig. 4).

There was no indication of intermediate structures **C** or **D** from the correlations in the ROESY spectrum. Peak integration[†] of the H1 and H9 to the HB correlations showed a ratio of 2:1 between intermediates **A** and **B**. However, the computational results reveal form **A** to be 1.45 kcal mol^{-1} higher in energy. The ratio of **A**:**B** will depend

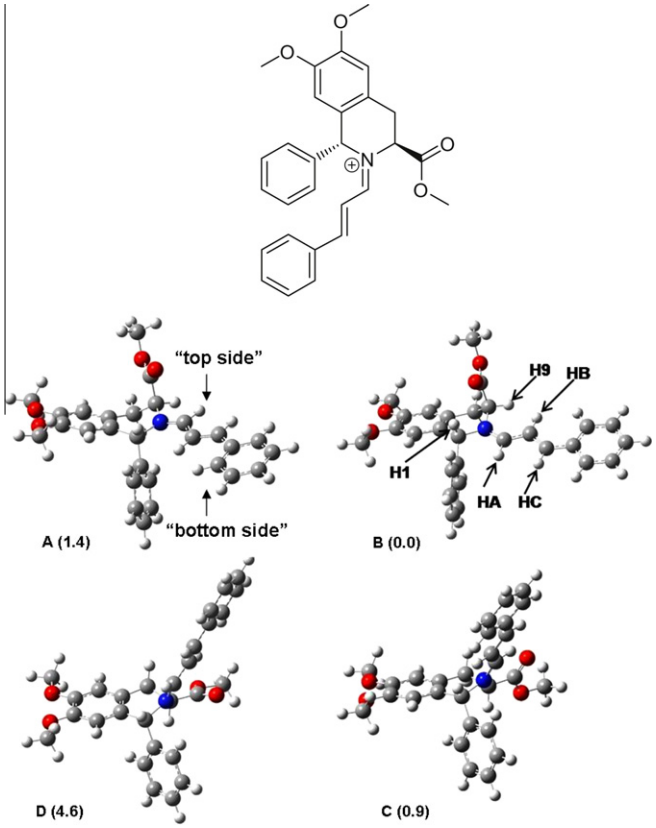

Figure 3. Optimized structures and relative energies (kcal mol^{-1}) of the iminium ion formed between cinnamaldehyde and catalyst **4** at the B3LYP/6-31+G(d) level of theory.

on the energy barrier leading to imine formation, suggesting that the product ratio (**A**:**B**) at room temperature is kinetically determined. Therefore, based on the NMR evidence and the results of the iminium intermediate computations, it was concluded that both

[†] Integration of the correlation dots on the ROESY spectrum was performed.

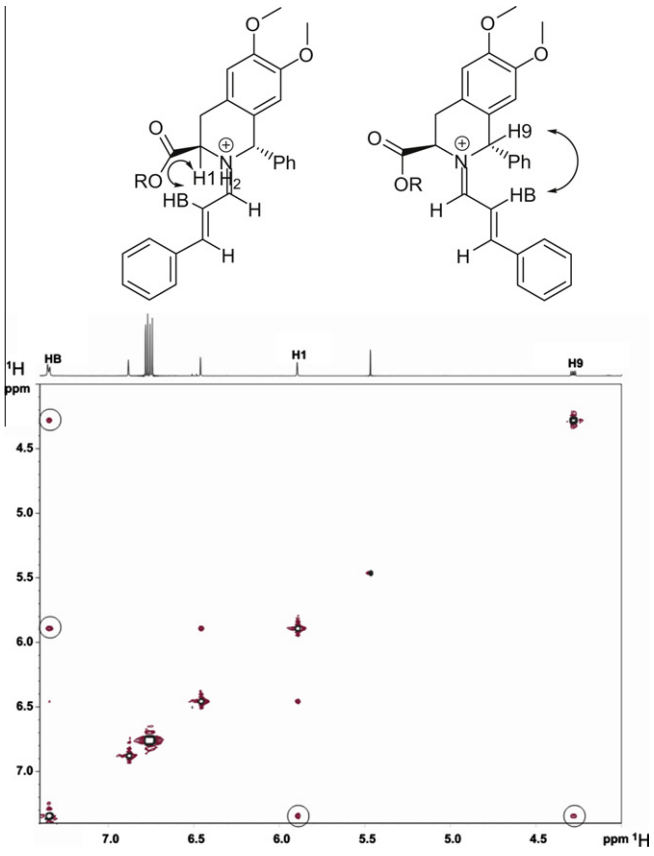

Figure 4. Expanded ROESY spectrum of catalyst **4** and cinnamaldehyde in CD_3CN at room temperature with characteristic cross-peaks marked.

iminium structures **A** (*E*)-isomer and **B** (*Z*)-isomer were present in solution at room temperature with the majority being the kinetically preferred structure **A**.

Another interesting observation from the NMR experiments was that the iminium proton HA was not seen at room temperature. However, proton signals HB and HC were clearly visible and confirmed using 2D NMR experiments which included HMBC, HSQC and COSY. These signals were clearly distinguished from the free form of cinnamaldehyde. Performing the ^1H NMR experiment at −38 °C showed the appearance of two broad peaks in the expected iminium proton region see Figure 5.

We concluded, that the iminium proton was in the intermediate exchange regime (μs to ms timescale) of a two-site exchange at room temperature and, therefore, only observable at a lower temperature (in this case −38 °C). This confirmed our initial room temperature result of the interconversion between structures **A** and **B**.

From the imine intermediates **A** and **B** (see Fig. 3), the course of the [2+4]-cycloaddition reaction was then studied computationally following the method reported by Houk et al.[41] Four possible modes of attack for the incoming cyclopentadiene on each imine intermediate exists. The first two products arise from 'top side' attack of cyclopentadiene on the imine (see Fig. 3) where one CH_2 group of cyclopentadiene is pointing out of the plane of the page (indicated with the symbol **I**) and the other one with the CH_2 pointing into the plane of the page (indicated as **II**). The second pair of products arise from the corresponding 'bottom side' attack. The eight transitions states were calculated and the energy profile for each intermediate is presented in Figure 6. Similar to the model proposed by the Houk group, our transition structures followed a 'concerted but very asynchronous pathway'.[41]

The experimentally observed products are in the following order: *exo*-(*R*), *endo*-(*R*), *exo*-(*S*) and *endo*-(*S*) (see Table 1 for the corresponding structures). It is clear from the activation energies that the reaction preferably proceeded through intermediate **A**. The transition state with the lowest energy barrier with respect to the imine intermediate **A** (TS-top-II) led to the major experimentally observed product. This observation agreed with our NMR study which confirmed the dominant presence of intermediate **A**. The competing reaction product was the *endo*-(*R*)-adduct. The transition state leading to that (TS-top-I) has the second lowest activation energy (15.5 kcal mol^{-1}—see Fig. 6). The presence of both (*E*)- and (*Z*)-isomers of the cinnamaldehyde/iminium ion complex is a contributing factor for the low enantioselectivity of the reaction products.

The theoretical observation that attack of the cyclopentadiene is from the top (A1-top-II) of the substrate, which corresponds to the lowest activation energy, enabled us to rationalize the results observed with catalysts **7**–**9** (Table 1, entries 7–9) as well. Although the iminium intermediate was forming with these catalysts (seen from ^1H NMR), the two phenyl rings at the C9 position will prevent attack of the diene from the top face, hence leading to the poor conversion.

3. Conclusion

For the first time an organocatalyst bearing a secondary nitrogen within a cyclohexane ring has been evaluated in the

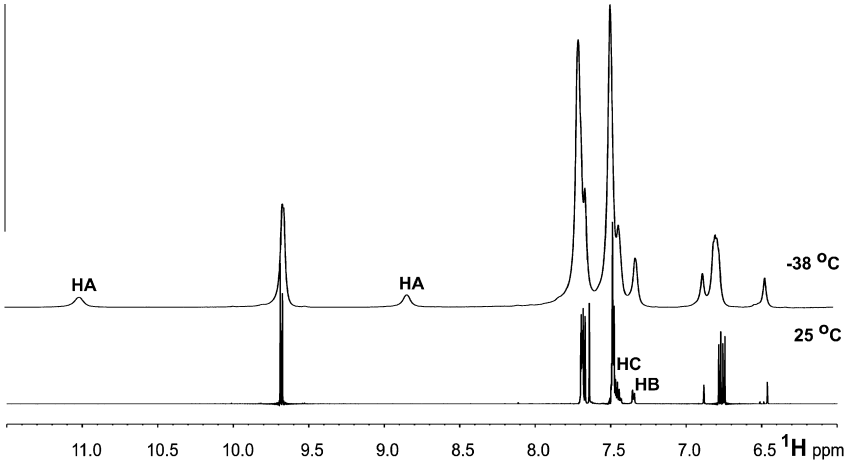

Figure 5. Expanded ^1H NMR spectrum of catalyst **4** and cinnamaldehyde in CD_3CN.

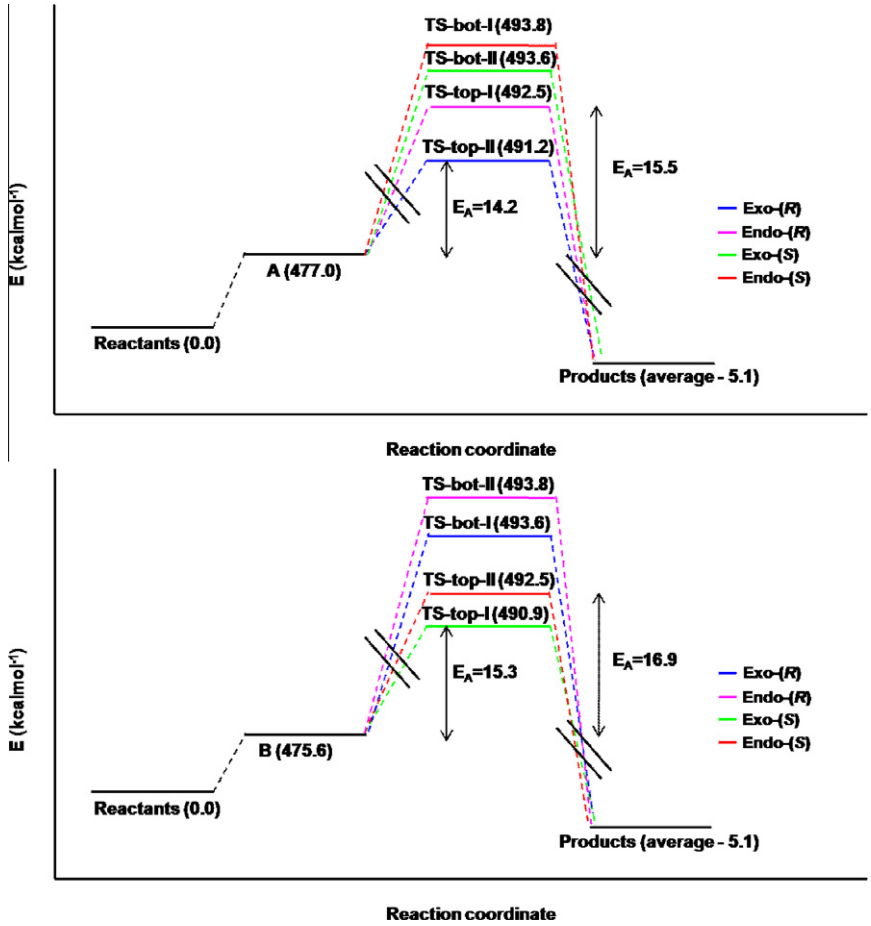

Figure 6. Calculated energy profiles for the catalysed Diels–Alder reaction for the pathways corresponding to imine intermediate **A** (top) and **B** (bottom), respectively.

asymmetric Diels–Alder reaction, thus leading to a new class of TIQ based organocatalysts. Catalyst **4** afforded good to excellent chemical conversion but poor selectivity with the addition of TfOH as the cocatalyst. Furthermore, detailed computational and NMR spectroscopic studies on the reaction intermediates and the reaction mechanism allowed us to rationalize the modest level of stereocontrol due to the presence of both (*E*)- and (*Z*)-isomers of the cinnamaldehyde and suggested how to design second generation catalysts. Studies into this class of organocatalysts are ongoing in our laboratory.

4. Experimental

4.1. General

Reagents and solvents were purchased from Aldrich, Merck and Fluka. All NMR spectra were recorded on Bruker AVANCE III 400 MHz or 600 MHz instrument at room temperature unless otherwise stated. Chemical shifts are expressed in ppm relative to TMS unless otherwise stated and coupling constants are reported in Hertz. Thin layer chromatography (TLC) was performed using Merck Kieselgel 60 F254 plates. Crude compounds were purified with column chromatography using silica gel (60–200 mesh). All solvents were dried using standard procedures. All IR spectra were recorded on a Perkin Elmer spectrum 100 instrument with a universal ATR attachment. Optical rotations were recorded on a Perkin Elmer Polarimeter. High resolution mass spectrometric data was obtained using a Bruker microTOF-Q II instrument operating at ambient temperatures. All melting points are uncorrected. The enantiomeric excess of the chiral Diels–Alder products was determined by gas chromatography Agilent 6890 GC-Ms with a Agilent 7683 auto injector system equipped with an Astec Chiraldex gamma-TA column (30 m × 0.25 mm), with helium gas as carrier gas and electron impact ionization (EI, 70 eV) or a Agilent 6820 capillary gas chromatograph with a CP-Chirasil-β-Dex column (25 m × 0.25 mm), nitrogen as carrier gas and a flame ionization detector.

4.2. Synthesis of (*S*)-1,2,3,4-tetrahydroisoquinoline-3-carboxylic acid 1

This compound was prepared by following the literature procedure from (*S*)-phenylalanine.[27]

4.3. Synthesis of (*S*)-methyl 1,2,3,4-tetrahydroisoquinoline-3-carboxylate 2

This compound was prepared by following the literature procedure from **1** which was in turn derived from (*S*)-phenylalanine.[27]

4.4. Synthesis of (1*R*,3*S*)-6,7-dimethoxy-1-phenyl-1,2,3,4-tetrahydroisoquinoline-3-carboxylic acid 3

This compound was prepared by following the literature procedure[28] from L-DOPA with a slight modification which we have recently reported.[22]

4.5. Synthesis of (1*R*,3*S*)-methyl-6,7-dimethoxy-1-phenyl-1,2,3,-4-tetrahydroisoquinoline-3-carboxylate 4

This compound was prepared by following the literature procedure from compound **3**.[28]

4.6. Synthesis of (1*R*,3*S*)-isopropyl-6,7-dimethoxy-1-phenyl-1,2,3,4-tetrahydroisoquinoline-3-carboxylate 5

To a stirred solution of compound **3** (1.00 g, 3.2 mmol) in dry isopropanol (100 ml) at 0 °C, thionyl chloride (4.6 ml, 64.8 mmol) was added dropwise. The mixture was then allowed to warm up to room temperature and stirred overnight. The solution was then concentrated in vacuo and the residue washed with sodium bicarbonate solution (50 ml) and extracted with ethyl acetate (2 × 25 ml). The organic extracts were combined and dried over anhydrous Na_2SO_4 and the solvent was removed in vacuo. The resulting residue was purified by column chromatography (50:50 EtOAc/Hexane, R_f 0.6) to afford the isopropyl TIQ ester 5 (0.95 g, 84%) as a solid. Melting point 73–75 °C. $[\alpha]_D^{20} = -70.0$ (*c* 0.12 in $CHCl_3$). IR (neat) ν_{max}: 2938, 1724, 1512, 1246, 1218, 1103, 702 cm^{-1}. HRMS calcd for $C_{21}H_{25}NO_4$ ($M+H^+$) 356.1856, found 356.1872. ^1H NMR (400 MHz, $CDCl_3$) δ = 7.39–7.11 (m, 5H), 6.67 (s, 1H), 6.34 (s, 1H), 5.26 (s, 1H), 5.02 (dq, *J* = 12.5, 6.3 Hz, 1H), 3.87 (s, 3H), 3.75 (dd, *J* = 8.6, 5.0 Hz, 1H), 3.68 (s, 3H), 3.14 (dd, *J* = 16.0, 5.0 Hz, 1H), 2.98 (dd, *J* = 16.0, 8.7 Hz, 1H), 1.37–1.09 (m, 6H). ^{13}C NMR (101 MHz, $CDCl_3$) δ = 172.90, 147.88, 147.40, 144.65, 128.71, 128.38, 128.05, 127.32, 125.87, 111.14, 110.83, 68.40, 58.89, 55.82, 51.42, 31.16, 21.82, 21.77.

4.7. Synthesis of (*S*)-methyl 6,7-dimethoxy-1,2,3,4-tetrahydroisoquinoline-3-carboxylate 6

This compound was prepared by following the literature procedure from L-DOPA.[30]

4.8. Synthesis of ((1*R*,3*S*)-6,7-dimethoxy-1-phenyl-1,2,3,4-tetrahydroisoquinolin-3-yl)diphenylmethanol 7

We recently reported the synthesis of this compound which is derived from compound **3**.[22]

4.9. Synthesis of (1*R*,3*S*)-6,7-dimethoxy-3-(methoxydiphenylmethyl)-1-phenyl-1,2,3,4-tetrahydroisoquinoline 8[32]

To a stirred solution of the *N*-benzyl protected derivative of compound **7** (0.50 g, 0.92 mmol) in dry THF (20 ml) was added sodium hydride (0.07 g, 3.0 mmol) at 0 °C under an inert atmosphere. The reaction mixture was then stirred for three hours at room temperature and then MeI (0.2 ml, 2.4 mmol) was added. The mixture was heated under reflux overnight. The excess NaH was hydrolysed with aqueous NH_4Cl solution. The organic layer separated and the aqueous layer extracted with ethyl acetate (2 × 10 ml). The organic extracts were combined and dried over anhydrous Na_2SO_4 and the solvent was removed in vacuo. The resulting residue was purified by column chromatography (30:70 EtOAc/Hexane, R_f 0.65) to afford the *N*-benzyl diphenyl methoxy derivative of compound **8** (0.40 g, 78%) as a yellow oil. $[\alpha]_D^{20} = -80.0$ (*c* 0.10, $CHCl_3$). IR (neat) ν_{max}: 2939, 1509, 1446, 1241, 1093, 1079, 695 cm^{-1}. HRMS calcd for $C_{38}H_{37}NO_3$ ($M+H^+$) 556.2846, found 556.2855. ^1H NMR (400 MHz, $CDCl_3$) δ = 7.28–7.00 (m, 18H), 6.96–6.89 (m, 2H), 6.77 (s, 1H), 6.31 (s, 1H), 4.68 (s, 1H), 4.22 (dd, *J* = 12.5, 3.4 Hz, 1H), 4.11–4.02 (m, 1H), 3.92 (s, 3H), 3.67 (s, 3H), 3.29–3.14 (m, 2H), 3.03–2.89 (m, 4H). ^{13}C NMR (101 MHz, $CDCl_3$) δ = 147.71, 147.48, 146.14, 145.51, 143.47, 140.22, 129.80, 129.06, 128.20, 128.12, 127.95, 127.70, 127.62, 127.04, 126.78, 126.73, 126.34, 126.31, 126.06, 125.53, 112.10, 111.59, 79.43, 64.65, 56.78, 55.84, 55.78, 51.60, 23.49.

The benzyl group was then removed following a procedure we have recently reported for the analogous compound **7** to yield compound **8** (0.2 g, 60%) as a white solid. Melting point 190–192 °C. $[\alpha]_D^{20} = -10.0$ (*c* 0.11, $CHCl_3$). IR (neat) ν_{max}: 2934, 1514, 1448, 1244, 1224, 1063, 698 cm^{-1}. HRMS calcd for $C_{31}H_{31}NO_3$ ($M+H^+$) 466.2377, found 466.2369. ^1H NMR (400 MHz, $CDCl_3$) δ = 7.47–7.12 (m, 12H), 7.08 (t, *J* = 7.6 Hz, 2H), 6.92 (d, *J* = 7.6 Hz, 2H), 6.65 (s, 1H), 6.40 (s, 1H), 5.23 (s, 1H), 3.95 (dd, *J* = 11.5, 3.6 Hz, 1H), 3.86 (s, 3H), 3.70 (s, 3H), 2.92–2.75 (m, 4H), 2.52 (dd, *J* = 16.2, 11.5 Hz, 3H). ^{13}C NMR (101 MHz, $CDCl_3$) δ = 147.83, 147.16, 143.92, 141.62, 140.86, 129.68, 129.40, 129.04, 128.40, 128.09, 127.41, 127.39, 127.30, 127.19, 127.18, 111.60, 110.51, 84.68, 59.96, 55.91, 55.81, 51.16, 49.48, 29.52.

4.10. Synthesis of (1*R*,3*S*)-3-(diphenyl(trimethylsilyl)methyl)-6,7-dimethoxy-1-phenyl-1,2,3,4-tetrahydroisoquinoline 9[32]

To a stirred solution of compound **7** (0.50 g, 1.1 mmol) and triethylamine (0.18 ml, 1.3 mmol) in dry dichloromethane (20 ml) trimethylsilyl triflate (0.24 ml, 1.33 mmol) was added dropwise at 0 °C under an inert atmosphere. The mixture was then allowed to warm up to room temperature and stirred overnight. The mixture was washed with water and the organic extracts were combined, dried over anhydrous Na_2SO_4 and the solvent was removed in vacuo. The resulting residue was purified by column chromatography (20:80 EtOAc/Hexane, R_f 0.55) to afford the diphenyl trimethylsilyl derivative **9** (0.52 g, 86%) as a white solid. Melting point 79–81 °C. $[\alpha]_D^{20} = -30.0$ (*c* 0.10, $CHCl_3$). IR (neat) ν_{max}: 2952, 1513, 1446, 1245, 1225, 1067, 834, 752, 698 cm^{-1}. HRMS calcd for $C_{33}H_{37}NO_3Si$ ($M+H^+$) 524.2615, found 524.2595. NMR chemical shifts are expressed in ppm relative to the $CHCl_3$ peak. ^1H NMR (400 MHz, $CDCl_3$) δ = 7.63–7.44 (m, 3H), 7.42–7.18 (m, 11H), 7.07 (d, *J* = 7.4 Hz, 2H), 6.73 (s, 1H), 6.58 (s, 1H), 5.40 (s, 1H), 4.08–3.92 (m, 4H), 3.85 (s, 3H), 2.71 (dd, *J* = 14.2, 11.1 Hz, 2H), -0.01 (s, 9H). ^{13}C NMR (101 MHz, $CDCl_3$) δ = 145.61, 144.90, 143.05, 142.41, 142.03, 127.19, 126.47, 125.94, 125.89, 125.39, 125.24, 125.07, 124.70, 124.67, 109.41, 108.34, 80.66, 57.98, 53.71, 53.61, 49.68, 27.11, −0.00.

4.11. General procedure for the Diels–Alder reaction

To a vial containing the catalyst (0.1 mmol) and the acid (0.1 mmol) in 457 μl of CH_3CN and 25 μl of H_2O was added the α,β-unsaturated aldehyde (1.0 mmol) followed by the diene (3.0 mmol). In the case of cyclopentadiene, it was freshly distiled before use. The reaction mixture was stirred for the time specified in the text. It was then diluted with Et_2O and washed successively with H_2O and brine. The organic layer was dried over anhydrous Na_2SO_4, and concentrated in vacuo. The resulting residue was purified by silica gel chromatography and analysed as described according to the following references Table 3, entry 1,[8] entry 2,[8] entry 3,[8] entry 4,[42] entry 5,[43] entry 6,[44] entry 7,[8] entry8.[8] Chromatographs and retention times for all chiral products were comparable to those reported.

4.12. NMR spectroscopy details

Study of the intermediate iminium ion structure. To a solution of **4** (5.0 mg, 0.015 mmol) and TfOH (1.4 μl, 0.015 mmol) in 475 μl of CD_3CN and 25 μl H_2O, (*E*)-cinnamaldehyde (9.6 μl, 0.075 mmol) and was added. 1D ^1H and ^{13}C experiments were recorded according to the standard Bruker library, using 16 and 1024 scans, respectively. 2D homonuclear COSY experiments and heteronuclear HSQC and HMBC experiments were recorded according

the standard Bruker library with 8 and 512; 8 and 256; and 16 and 512 scans and number of complex points in f1 dimension, respectively. 2D homonuclear. ROESY experiments were recorded according to Thiele et al., with 40 scans and 512 complex points.[45] A mixing time of 250 ms was applied to achieve proper transfer and a relaxation delay of 2 s was applied, when distances where extracted. ROE distances were used as a range from 2.5 to 5 Å for calculations to restrain.

4.13. Computational details

Complexes **A**–**D** and transitions states were optimized in the gas phase using GAUSSIAN 09[46] at the the density functional theory (DFT) level employing the B3LYP (Becke's three-parameter non-local exchange function[47–49]) with the correlation functional of Lee, Yang and Par[50] in conjunction with the 6-31+G(d) basis set. set. Diffuse functions are typically used for a more accurate description where lone pair electrons are involved, while polarization functions remove some limitations of the basis set by expansion of the virtual space. Solvation effects were not considered in order to simplify the model. Geometry optimizations were performed without restrictions in order to locate extrema presented herein. Frequency calculations were performed for all structures. Transitions states were characterized by a single imaginary frequency, which corresponds to the movement of atoms consistent with the expected reaction. To ensure that the lowest energy transition state for the first step (bond formation between atoms 1 and 2 in Figure 6) was found, a relaxed scan (using a semi-empirical calculation with Parameterized Model number 6)[51] was performed with the atom distance for atoms 1 and 2 kept fixed at about 1.89 Å. The scan entailed a 360° rotation of the cyclopentadiene molecules in 15° steps. The structure corresponding to the lowest energy structure on the energy profile was used for a normal unconstrained transition state for the DFT calculation.

Acknowledgements

The authors wish to thank the National Research Foundation (South Africa, GUN 65387) The SA/Swedish Research Links Programme grant and Aspen Pharmacare, South Africa.

References

1. *Enantioselective Organocatalysis*; Dalko, P. I., Ed.; Wiley-VCH Verlag Gmb & Co KGaA: Weinheim, 2007.
2. Dondoni, A.; Massi, A. *Angew. Chem., Int. Ed.* **2008**, *47*, 4638–4660.
3. Melchiorre, P.; Marigo, M.; Carlone, A.; Bartoli, G. *Angew. Chem., Int. Ed.* **2008**, *47*, 6138–6171.
4. Erkkila, A.; Majander, I.; Pihko, P. M. *Chem. Rev.* **2007**, *107*, 5416–5470.
5. Lelais, G.; MacMillan, D. W. C. *Aldrichim. Acta* **2006**, *39*, 79–87.
6. List, B. *Chem. Commun.* **2006**, 819–824.
7. Mukherjee, S.; Yang, J. W.; Hoffmann, S.; List, B. *Chem. Rev.* **2007**, *107*, 5471–5569.
8. Ahrendt, K. A.; Borths, C. J.; MacMillan, D. W. C. *J. Am. Chem. Soc.* **2000**, *122*, 4243–4244.
9. Franzen, J.; Marigo, M.; Fielenbach, D.; Wabnitz, T. C.; Kjaersgaard, A.; Jorgensen, K. A. *J. Am. Chem. Soc.* **2005**, *127*, 18296–18304.
10. List, B.; Lerner, R. A.; Barbas, C. F. *J. Am. Chem. Soc.* **2000**, *122*, 2395–2396.
11. Liu, Z.-Z.; Wang, Y.; Tang, Y.-F.; Chen, S.-Z.; Chen, X.-G.; Li, H.-Y. *Bioorg. Med. Chem. Lett.* **2006**, *16*, 1282–1285.
12. Scott, J. D.; Williams, R. M. *Chem. Rev.* **2002**, *102*, 1669–1730.
13. Tarver, J. E.; Pfizenmayer, A. J.; Joullié, M. M. *J. Org. Chem.* **2001**, *66*, 7575–7587.
14. Zarranz De Ysern, M. E.; Ordoñez, L. A. *Prog. Neuro-Psychopharmacol.* **1981**, *5*, 343–355.
15. Arvidsson, P. I.; Govender, T.; Kruger, H. G.; Maguire, G. E. M.; Naicker, T. *S. Afr. J. Chem.* **2009**, *62*, 60–66.
16. Boyle, G. A.; Govender, T.; Kruger, H. G.; Maguire, G. E. M. *Tetrahedron: Asymmetry* **2004**, *15*, 3775–3781.
17. Boyle, G. A.; Govender, T.; Kruger, H. G.; Maguire, G. E. M. *Tetrahedron: Asymmetry* **2004**, *15*, 2661–2666.
18. Basavaiah, D.; Das, U.; Roy, S. *J. Chem. Sci.* **2009**, *121*, 1003–1010.
19. Blanc, C.; Hannedouche, J.; Agbossou-Niedercorn, F. *Tetrahedron Lett.* **2003**, *44*, 6469–6473.
20. Hari, Y.; Sakuma, M.; Miyakawa, A.; Hatano, K.; Aoyama, T. *Heteroycles* **2008**, 305–311.
21. Stingl, K.; Martens, J.; Wallbaum, S. *Tetrahedron: Asymmetry* **1992**, *3*, 223–226.
22. Chakka, S. K.; Andersson, P. G.; Maguire, G. E. M.; Kruger, H. G.; Govender, T. *Eur. J. Org. Chem.* **2010**, 972–980.
23. Peters, B. K.; Chakka, S. K.; Naicker, T.; Maguire, G. E. M.; Kruger, H. G.; Andersson, P. G.; Govender, T. *Tetrahedron: Asymmetry* **2010**, *21*, 679–687.
24. Kawthekar, R. B.; Chakka, S. K.; Francis, V.; Andersson, P. G.; Kruger, H. G.; Maguire, G. E. M.; Govender, T. *Tetrahedron: Asymmetry* **2010**, *21*, 846–852.
25. Chakka, S. K.; Peters, B. K.; Maguire, G. E. M.; Kruger, H. G.; Andersson, P. G.; Govender, T. *Tetrahedron: Asymmetry* **2010**.
26. List, B. *Synth. Lett.* **2001**, 1675–1686.
27. Grunewald, G. L.; Sall, D. J.; Monn, J. A. *J. Med. Chem.* **1988**, *31*, 824–830.
28. Aubry, S.; Pellet-Rostaing, S.; Faure, R.; Lemaire, M. *J. Heterocycl. Chem.* **2006**, *43*, 139–148.
29. Cai, T. B.; Zou, A.; Thomas, J. B.; Brieaddy, L.; Navarro, H. A.; Carrol, F. I. *J. Med. Chem.* **2008**, 1849–1860.
30. Tang, Y. F.; Liu, Z. Z.; Chen, S. Z. *Tetrahedron Lett.* **2003**, *44*, 7091–7094.
31. Palomo, C.; Mielgo, A. *Angew. Chem., Int. Ed.* **2006**, *45*, 7876–7880.
32. Aggarwal, V. K.; Sandrinelli, F.; Charmant, J. P. H. *Tetrahedron: Asymmetry* **2002**, *13*, 87–93.
33. Hartikka, A.; Hojabri, L.; Bose, P. P.; Arvidsson, P. I. *Tetrahedron: Asymmetry* **2009**, *20*, 1871–1876.
34. Lemay, M.; Ogilvie, W. W. *Org. Lett.* **2005**, *7*, 4141–4144.
35. Groselj, U.; Schweizer, W. B.; Ebert, M.-O.; Seebach, D. *Helv. Chim. Acta* **2009**, *92*, 1–13.
36. Groselj, U.; Seebach, D.; Badine, D. M.; Schweizer, W. B.; Beck, A. K.; Krossing, I.; Klose, P.; Hayashi, Y.; Uchimaru, T. *Helv. Chim. Acta* **2009**, *92*, 1225–1259.
37. Seebach, D.; Gilmour, R.; Groselj, U.; Deniau, G.; Sparr, C.; Ebert, M.-O.; Beck, A. K.; McCusker, L. B.; Sisak, D.; Uchimaru, T. *Helv. Chim. Acta* **2010**, *93*, 603–634.
38. Seebach, D.; Groselj, U.; Badine, D. M.; Schweizer, W. B.; Beck, A. K. *Helv. Chim. Acta* **2008**, *91*, 1999–2034.
39. Naicker, T.; Govender, T.; Kruger, H. G.; Maguire, G. E. M. *Acta Crystallogr., Sect. E: Struct. Rep.* **2010**, *66*, 0638.
40. Naicker, T.; McKay, M.; Govender, T.; Kruger, H. G.; Maguire, G. E. M. *Acta Crystallogr., Sect. E: Struct. Rep.* **2009**, *65*, o3278.
41. Gordillo, R.; Houk, K. N. *J. Am. Chem. Soc.* **2006**, *128*, 3543–3553.
42. Kano, T.; Tanaka, Y.; Maruoka, K. *Org. Lett.* **2006**, *8*, 2687–2689.
43. Gotoh, H.; Hayashi, Y. *Org. Lett.* **2007**, *9*, 2859–2862.
44. He, H.; Pei, B. J.; Chou, H.; Tian, T.; Cha, W. H.; Lee, A. W. M. *Org. Lett.* **2008**, *10*, 2421–2424.
45. Thiele, C. M.; Petzold, K.; Schleucher, J. *Chem. Eur. J.* **2009**, *15*, 585–588.
46. Frisch, M. J.; Trucks, G. W.; Schlegel, H. B.; Scuseria, G. E.; Robb, M. A.; Cheeseman, J. R.; Scalmani, G.; Barone, V.; Mennucci, B.; Petersson, G. A.; Nakatsuji, H.; Caricato, M.; Li, X.; Hratchian, H. P.; Izmaylov, A. F.; Bloino, J.; Zheng, G.; Sonnenberg, J. L.; Hada, M.; Ehara, M.; Toyota, K.; Fukuda, R.; Hasegawa, J.; Ishida, M.; Nakajima, T.; Honda, Y.; Kitao, O.; Nakai, H.; Vreven, T.; Montgomery, J. A., Jr.; Peralta, J. E.; Ogliaro, F.; Bearpark, M.; Heyd, J. J.; Brothers, E.; Kudin, K. N.; Staroverov, V. N.; Kobayashi, R.; Normand, J.; Raghavachari, K.; Rendell, A.; Burant, J. C.; Iyengar, S. S.; Tomasi, J.; Cossi, M.; Rega, N.; Millam, N. J.; Klene, M.; Knox, J. E.; Cross, J. B.; Bakken, V.; Adamo, C.; Jaramillo, J.; Gomperts, R.; Stratmann, R. E.; Yazyev, O.; Austin, A. J.; Cammi, R.; Pomelli, C.; Ochterski, J. W.; Martin, R. L.; Morokuma, K.; Zakrzewski, V. G.; Voth, G. A.; Salvador, P.; Dannenberg, J. J.; Dapprich, S.; Daniels, A. D.; Farkas, Ö.; Foresman, J. B.; Ortiz, J. V.; Cioslowski, J.; Fox, D. J. *GAUSSIAN 09 Revision A. 1*; Gaussian, Inc.: Wallingford CT, 2009.
47. Becke, A. D. *J. Chem. Phys.* **1992**, *97*, 9173–9177.
48. Becke, A. D. *J. Chem. Phys.* **1992**, *96*, 2155–2160.
49. Becke, A. D. *J. Chem. Phys.* **1993**, *98*, 5648–5652.
50. Lee, C.; Yang, W.; Parr, R. G. *Phys. Rev. B* **1988**, *37*, 785.
51. Stewart, J. J. P. *J. Mol. Model.* **2007**, *13*, 1173–1213.